Article

Not peer-reviewed version

Influence of Ambient Pressure on the Jet-Ignition Combustion Performance and Flame Propagation Characteristics in a Constant Volume Combustion Chamber

Zongjie HU , Minglong LI , Xinke MIAO , Zhiyu WANG , Yuanzhi TANG , Xijiang WU , Wangchao YU , Zhe KANG , Jun DENG *

Posted Date: 24 May 2024

doi: 10.20944/preprints202405.1648.v1

Keywords: Pre-chamber; Jet ignition; Constant volume combustion chamber; Ambient pressure; Flame visualization

Article

Influence of Ambient Pressure on the Jet-Ignition Combustion Performance and Flame Propagation Characteristics in a Constant Volume Combustion Chamber

Zongjie HU [1], Minglong LI [1], Xinke MIAO [1], Zhiyu WANG [2], Yuanzhi TANG [1], Xijiang WU [2], Wangchao YU [1], Zhe KANG [3,4], Jun DENG [1,*]

[1] School of Automotive Studies, Tongji University, Shanghai 201804, China' zongjie-hu@tongji.edu.cn (Z.H.); 2011671@tongji.edu.cn (M.L.); miaoxinke@tongji.edu.cn (X.M.); tangyuanzhi121@163.com (Y.T.); 2133521@tongji.edu.cn (W.Y.);

[2] SAIC Motor Corporation Limited, Shanghai 201804, China; wangzhiyu@saicmotor.com (Z.W.); wuxijiang@saicmotor.com (X.W.);

[3] College of Mechanical and Vehicle Engineering, Chongqing University, Chongqing, China; zhekang@cqu.edu.cn

[4] State Key Laboratory of Mechanical Transmission for Advanced Equipments, Chongqing, China

* Correspondence: eagledeng@tongji.edu.cn; Tel.: 13701745052

Abstract: Based on a constant volume combustion chamber, the initial ambient pressure effect on combustion performance and flame propagation of the active and passive pre-chamber ignition systems were studied. Compared with the passive pre-chamber, the active pre-chamber can significantly expand the lean combustion limit, enhance the ignition and combustion performance, and speed up the combustion of the main combustion chamber. At slightly lean combustion conditions, the heat release performance has a positive correlation with the initial ambient pressure. As the premixed λ increases, the heat release performance and the initial ambient pressure begin to become negatively correlated. Ignition delay can be minimized by controlling the excess air coefficient in the pre-chamber close to the stoichiometric ratio. The high ambient pressure in the constant volume chamber greatly reduces the mixture entrainment ability of the jet flame at lean combustion conditions, thereby reducing the combustion speed and peak heat release rate.

Keywords: pre-chamber, jet ignition, constant volume combustion chamber, ambient pressure, flame visualization

1. Introduction

Under the target of "Carbon Peak" and "Carbon Neutral", hybrid electric vehicles (HEV) are increasingly favored by enterprises and consumers because of their fuel-electric synergistic technology, which offers good fuel efficiency and low emissions while considering the range of vehicles. Compared with stoichiometric combustion, lean combustion can improve the specific heat ratio of the mixture [1-4], resulting in improved engine thermal efficiency. Still, it faces the challenges of ignition difficulty and low flame propagation. The pre-chamber ignition system is recognized as one of the most reliable methods to achieve lean combustion [5].

The existing pre-chamber jet ignition method includes active pre-chamber and passive pre-chamber, while the active pre-chamber has been proved to achieve ultra-lean mixture combustion with lambda (λ) greater than 2.0 [6]. Compared with the active pre-chamber, the passive pre-chamber does not significantly improve the lean-combustion limit [7]. This is mainly due to insufficient scavenging inside the pre-chamber, making it difficult for the mixture near the spark plug electrode to achieve optimal ignition conditions. At the same time, the peak temperature of the mixture after

 doi:10.20944/preprints202405.1648.v1

ignition is relatively low at lean combustion conditions, the NOx emissions will be significantly reduced [8,9], even closing the zero level (<10 ppm) [10]. According to research by Jamrozik et al. [6], it could achieve a small non-repeatability of cycles and low NOX emissions ultra-lean combustion.

Changes in engine load mainly affect the ambient density and pressure inside the cylinder, which directly affect the flame propagation in the space. The in-cylinder flame formed by jet ignition propagates is similar to the fuel-air entrainment of the premix combustion [11]. The turbulent flame front induced by the flame jet develops outward and consumes the surrounding mixture. The amount of jet flame entrainment is the main factor affecting jet ignition performance [12]. The speed of the jet flame will increase as the ambient pressure increases [13], but it will not significantly affect the laminar flame stability [14]. Meanwhile, the low-flow injection inside the pre-chamber is mainly determined by injection pressure, timing and duration. Building a mixture with a suitable equivalence ratio distribution in the pre-chamber before the spark plug ignition is the prerequisite for optimizing jet ignition performance.

In this paper, based on a constant-volume combustion chamber (CVCC), the influence of different initial ambient pressures and lambda on flame propagation and the combustion characteristics of active/passive pre-chamber (APC/PPC) were studied.

2. Experimental setup

2.1 Pre-chamber design & experiment operating conditions

Figure 1 shows the schematic of the pre-chamber (PC), with a narrow bottom and six jet nozzles, forming an angle of 45° with the horizontal direction. The total volume in the pre-chamber is about 2.7 cm^3.

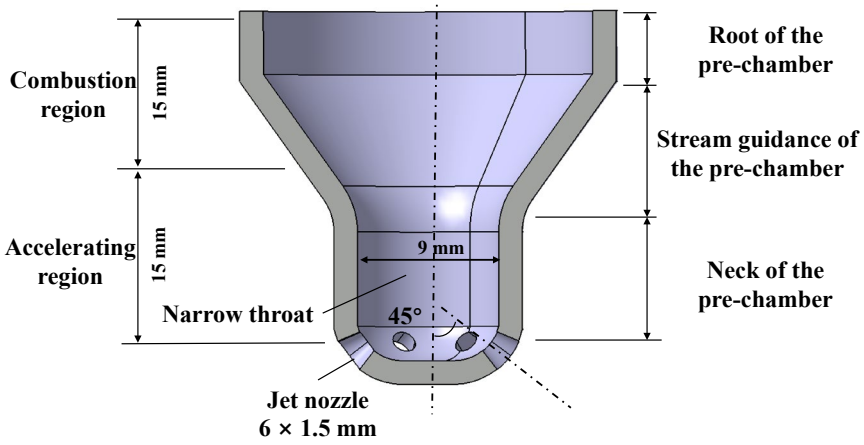

Figure 1. Pre-chamber structure design.

Figure 2 shows the constant-volume combustion chamber system, including a cylindrical CVCC, high-pressure gasoline injection system, spark ignition system, high-frequency pressure measurement system, and high-speed photography system. The combustion chamber of the CVCC is a horizontal Φ80×132mm cylinder. One end of the CVCC is equipped with optical quartz glass, the other end is equipped with a steel cover installed the pre-chamber.

The control system of ignition and injection is developed in-house using NI Compact RIO and LabVIEW. The pressure data acquisition system consists of a pressure sensor (Kistler 6115CF-4CQ07-4-1), a charge amplifier (Kistler 5064), and a computer with a data acquisition LabVIEW program. The spark and flame development are directly captured by a high-speed photography system, which includes a high-speed camera (Phantom VEO 610) and a computer with camera control software. The camera is synchronously triggered with the spark ignition. The high-pressure injection system includes a gasoline tank, a fuel pump, a low-flow PC injector and a main chamber (MC) injector. The initial ambient pressure inside the CVCC is controlled through a pressure-reducing valve and pressure gauge.

 doi:10.20944/preprints202405.1648.v1

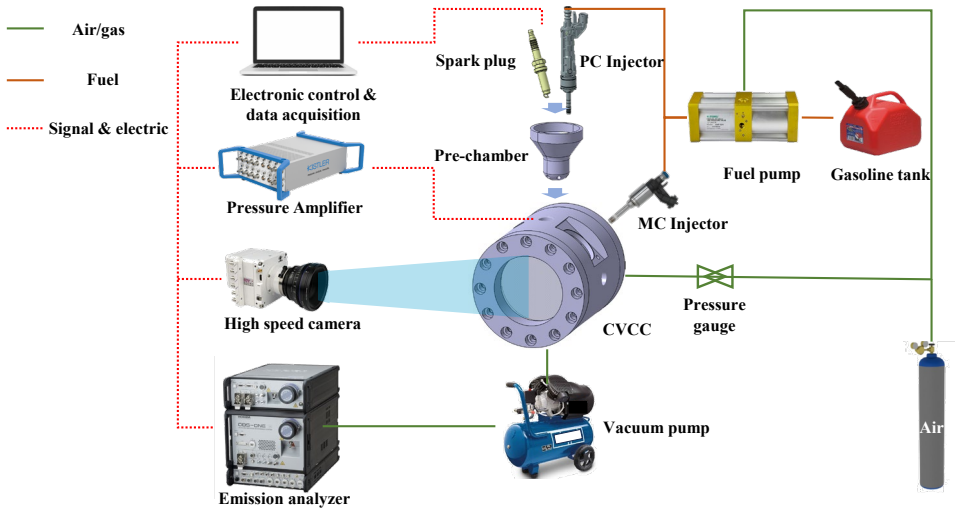

Figure 2. CVCC experiment system layout.

Table 1 shows the detailed experimental operating parameters. The injector in the pre-chamber maintains a minimum stable injection duration corresponding to 0.64 mg. The premixed λ is experimentally in a gradient of 0.1 from stoichiometric combustion to the lean limit of different jet ignition methods.

Table 1. Detailed operating conditions

Parameter	Value
Fuel	RON95
Premix λ	From 1.0 to the lean-limit
Initial ambient pressure P_a [MPa]	0.5, 0.75 & 1.0
Initial temperature T [K]	373
Low-flow injection mass in APC [mg]	0.64
Gasoline injection pressure [MPa]	20
Spark plug ignition energy [mJ]	120
Frames per second [fps]	10000
Image resolution [pixels]	560×516

Figure 3 shows the gasoline mixture preparation and signal control during the experiment. To ensure that the gasoline fuel is relatively uniformly mixed in the main chamber of CVCC, the CVCC is heated to 373K before the experiment, and then a sufficient amount of fuel is injected in the premixing stage by MC injector according to the premixed λ, initial ambient temperature and pressure, subsequently the corresponding mass of air is charged and left more than 180 seconds as premix interval. The spark delay in the PC is set at 1 ms.

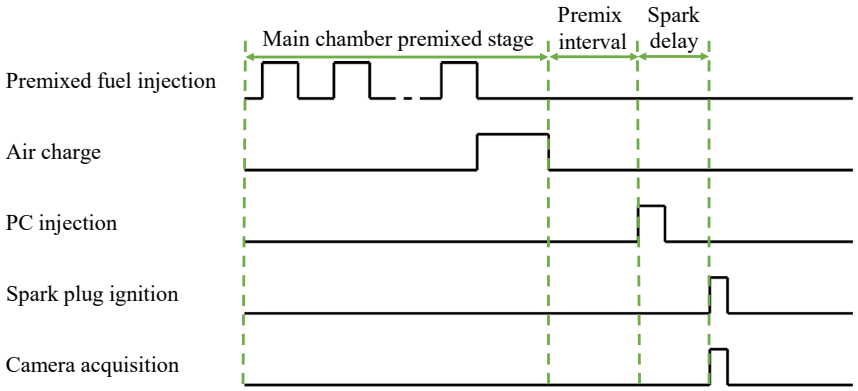

Figure 3. Gas mixture preparation and ignition control signal.

 doi:10.20944/preprints202405.1648.v1

2.2 Combustion performance parameters

Since the total amount of fuel differs at different λ and ambient pressure conditions, the calculated integral heat release is challenging to evaluate intuitively. The heat release rate of CVCC is calculated using the isentropic index algorithm that ignores the heat exchange of the chamber. As shown in Equation 1, the calculated heat release result is lower than the actual heat release.

$$Q_i = \frac{1}{\kappa - 1} \cdot [V \cdot (P_{i+1} - P_i)] \quad (1)$$

κ is the polytropic coefficient, P is the pressure and V is the volume of the CVCC.

The integral heat release (IHR) is the integral of Q_i by time, and 5% IHR is defined as the ignition delay period, and 5% to 90% IHR is defined as the main combustion period.

The premixing time in the CVCC is long enough. It can be considered that the gasoline fuel in the chamber is premixed homogeneously. The theoretical PC excess air coefficient can be calculated by referring to the method of Shah et al.[15], as shown in Equation 2 below:

$$\lambda_{PC} = \lambda_{MC} \cdot \frac{m_{MC} \cdot R_V}{m_{MC} \cdot R_V + m_{PC}} \quad (2)$$

Where R_V is the volume ratio of the PC and MC, m_{MC} is the premixed fuel mass in the MC, m_{PC} is the low-fuel mass injected into the PC.

According to a large number of research results, the combustion efficiency of lean combustion is generally higher than that of stoichiometric combustion [16]. Therefore, this article uses the heat release change ratio R_{HR} to evaluate the heat release at different premixed λ conditions, calculated according to the proportion of stoichiometric combustion, as shown in Equation 3.

$$R_{HR} = \left(\frac{Q}{Q_{sto}} \times \frac{m_{sto}}{m} - 1\right) \times 100\% \quad (3)$$

Q is the integral heat release calculated from a specific operating condition, m is the actual fuel injection amount at the working condition, Q_{sto} is the integral heat release at stoichiometric combustion conditions, and m_{sto} is the fuel injection mass at stoichiometric combustion conditions.

2.3 Jet flame analysis method

The flame propagation process generally includes jet flames in six different directions in the 6-hole pre-chamber. To evaluate the axial propagation of the jet flame along the jet nozzle direction, the average jet flame penetration length $\overline{X}$ can be calculated using all collected flame jet lengths.

$$\overline{X} = \frac{1}{6} \times \sum_{1}^{6} X' \quad (4)$$

Where the X' refers to the jet length in the axis direction of all orifices in the flame image plane. In addition, according to the flame area change of the jet flame propagation in the optical window, the flame jet area of the equivalent average jet penetration length at any moment can be calculated, as shown in Figure 4.

Preprints.org (www.preprints.org) | NOT PEER-REVIEWED | Posted: 24 May 2024 doi:10.20944/preprints202405.1648.v1

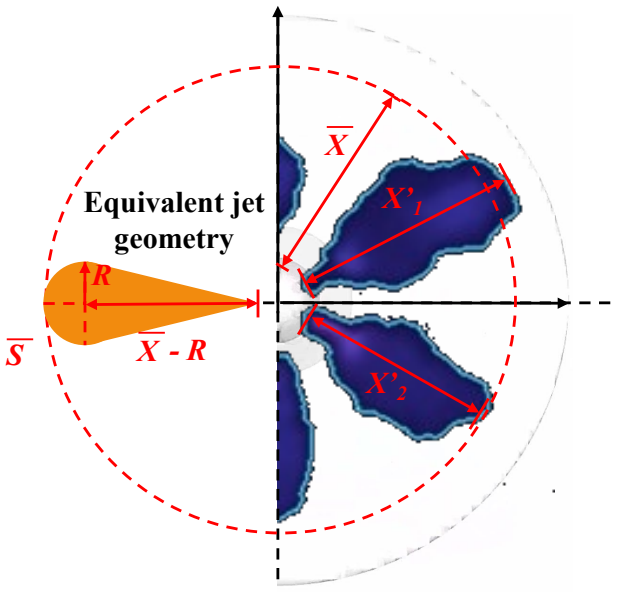

Figure 4. Jet flame geometry and equivalent jet geometry.

The geometric development of flame jet is similar to the entrainment of spray and fuel-premixed combustion. Its geometric shape can be approximated as a combination of triangle and semicircle [32], as shown in Equation 5.

$$\overline{S} = (\frac{\pi}{2} - 1)\ R^2 - \overline{X} \bullet R = \frac{1}{6} \times S \tag{5}$$

S is the cumulative flame area obtained by image post-processing, and R is the approximate spherical radius. The equivalent jet flame volume V_{Jet} can be obtained by Equation 6.

$$V_{Jet} = \frac{\pi R^2 \bullet (X' - R) + 2\pi R^3}{3} \tag{6}$$

The volume of the flame jet represents the gas amount of the flame entrainment, and the entrainment ratio Φ can be defined as the percentage change rate of the jet flame volume at different ambient pressure conditions [17] by Equation 7.

$$\Phi = \frac{(V_{Jet} - V_{Jet0})}{V_{Jet0}} \times 100\% \tag{7}$$

Where V_{Jet0} is the jet flame volume of stoichiometric combustion at 0.5 MPa initial ambient pressure.

3. Results and discussion

3.1 Combustion pressure and heat release rate

Figure 5 shows the combustion pressure and heat release rate of stoichiometric combustion and lean combustion of PPC at different ambient pressures. Figure 6 shows the combustion characteristics of PPC with different λ at different ambient pressures. The increase of premixed fuel causes the maximum pressure and integral heat release to increase with the increase of initial ambient pressure. It could be found from Figure 5 and Figure 6 that as premixed λ increases at high ambient pressure, the combustion performance decreases sharply, and the peak heat release rate decreases rapidly compared with low ambient pressure. The peak heat release rate at 1.0 MPa ambient pressure is reduced to the minimum when λ=1.1 as the turning point showing. The integral heat release change ratio R_{HR} is only higher than the stoichiometric combustion condition at lean combustion condition with 0.5 MPa ambient pressure. With 0.75 MPa and 1.0 MPa initial ambient pressures, R_{HR} decreases as λ increases. At the same time, Lean combustion will reduce the flame propagation speed and slow

 doi:10.20944/preprints202405.1648.v1

down the intensity of combustion heat release. The heat release curve gradually becomes flat, and misfire occurs at 1.0 MPa ambient pressure of λ=1.2.

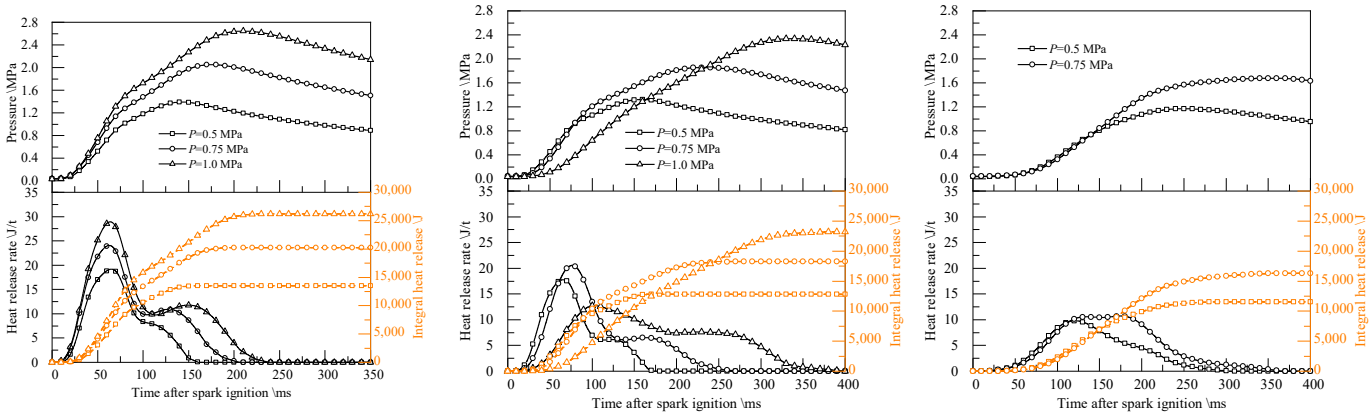

(a) λ=1.0 (b) λ=1.1 (c) λ=1.2

Figure 5. Combustion pressure & heat release rate of different premixed λ.

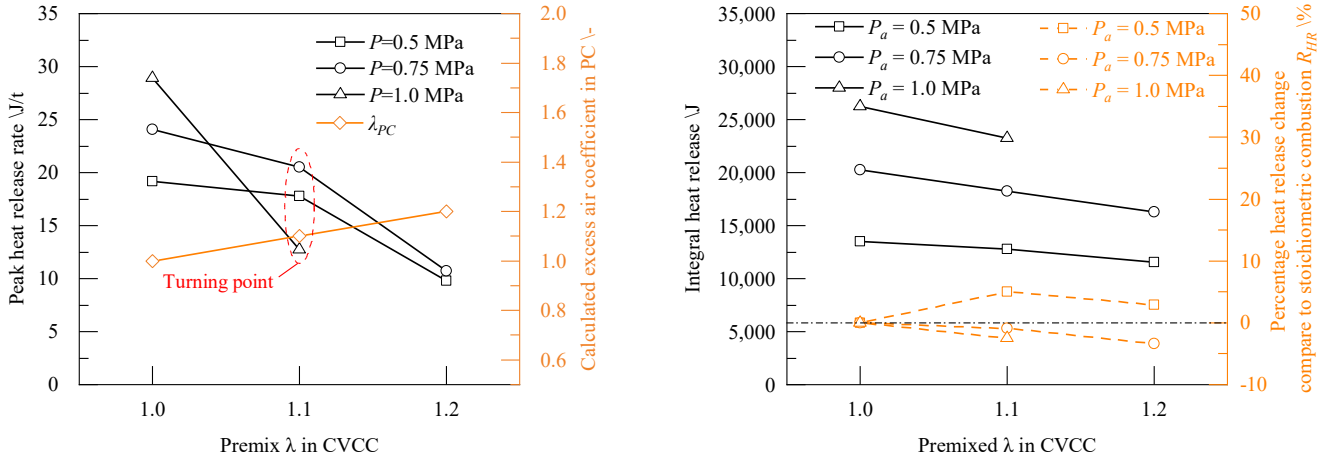

(a) Peak heat release (b) Integral heat release

Figure 6. Peak & integral heat release of PPC.

Figure 7 shows the changes in the ignition delay period and main combustion period of PPC at different premixed λ at different initial ambient pressures. The ignition delay at different initial ambient pressures with stoichiometric combustion is consistent, indicating that the ignition delay is not significantly related to the ambient pressure at the stoichiometric ratio. The initial ambient pressure increase in the pre-chamber makes the ignition delay and main combustion period significantly prolonged, which may be due to the flame propagation speed in the PPC reducing with the increase of premixed λ.

 doi:10.20944/preprints202405.1648.v1

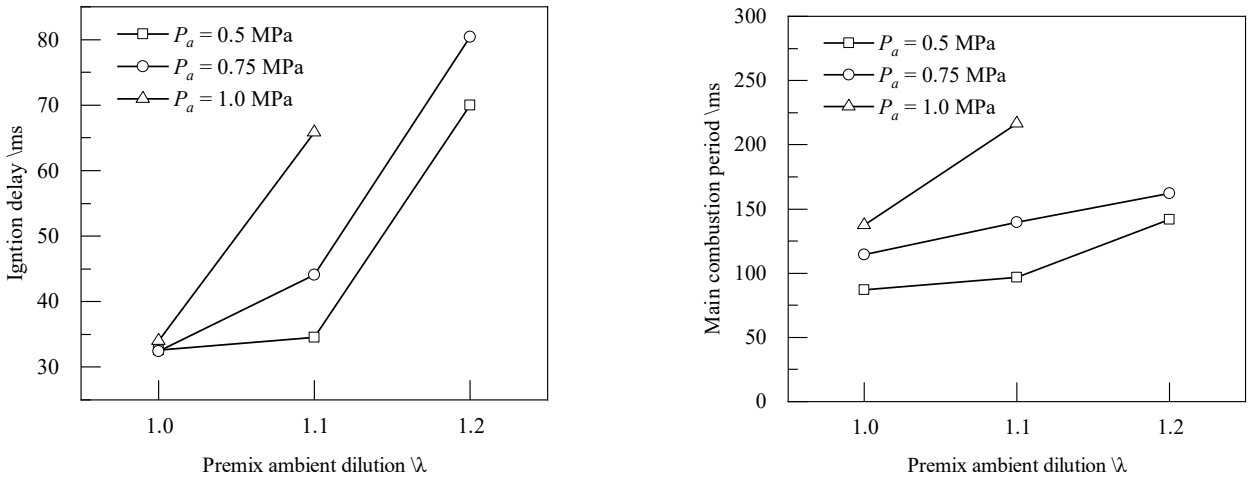

(a) Igntion delay (b) Combustion period

Figure 7. Combustion period of PPC.

Figure 8 shows the combustion pressure and heat release rate curves of APC. With the additional low-flow injection in the PC to improve the performance of the jet ignition system, the lean-combustion limit is expanded from λ=1.2 to λ=1.5 compared to those mentioned above in the PPC system. At the stoichiometric conditions of the APC and the slightly lean condition (λ=1.1), the combustion heat release performance of high ambient pressure is still better than that of low ambient pressure, and the peak heat release rate increases with the increase of ambient pressure, and there is a two-stage heat release period. Starting from λ=1.2, the negative impact of the initial ambient pressure in CVCC on jet ignition and flame propagation performance, the peak heat release decreases and the timing of peak heat release delays with the increase of λ. At the same time, the heat release only has one period when λ is over 1.2.

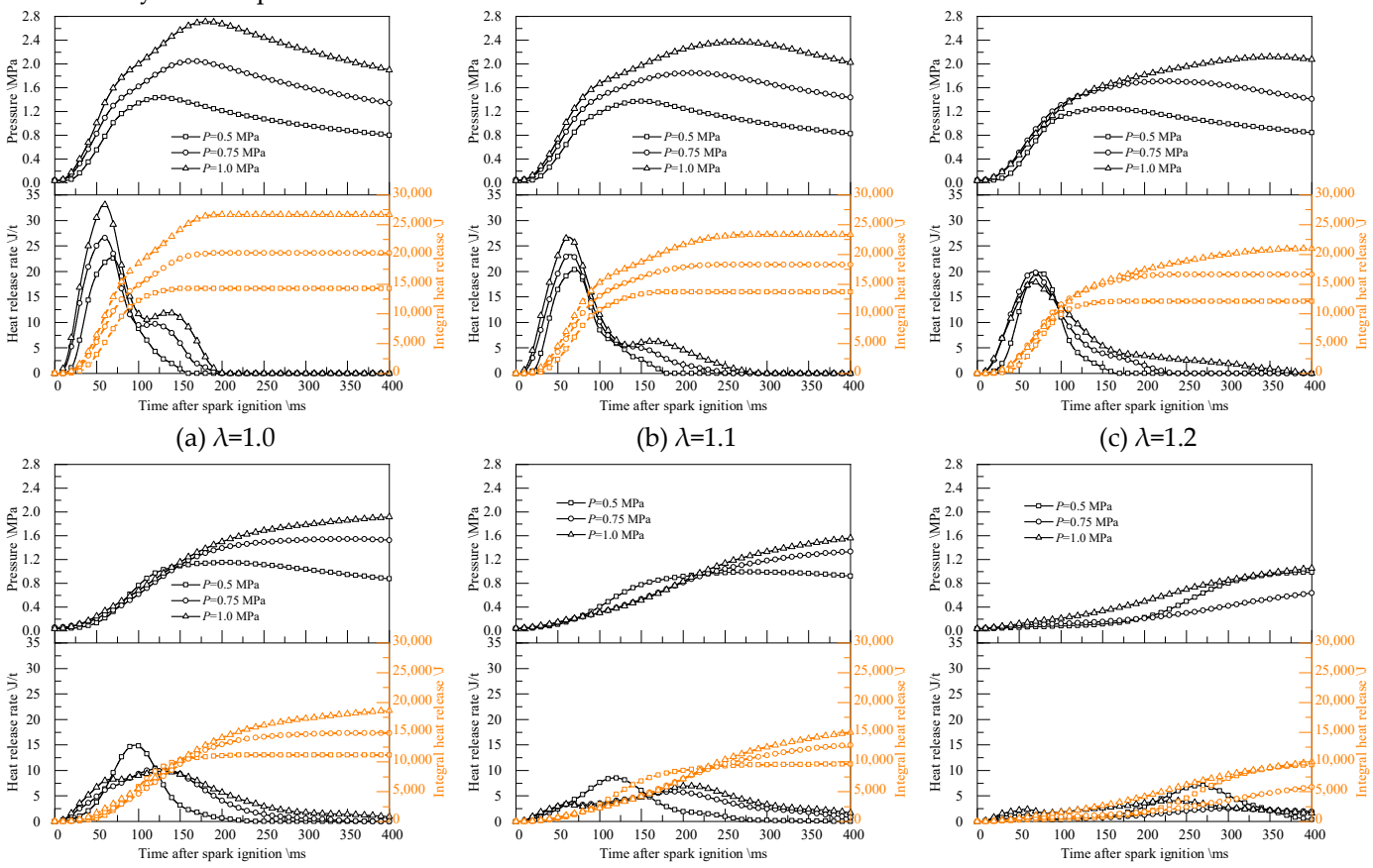

(a) λ=1.0 (b) λ=1.1 (c) λ=1.2

(d) λ=1.3 (e) λ=1.4 (f) λ=1.5

 doi:10.20944/preprints202405.1648.v1

Figure 8. Pressure & heat release at different premixed λ.

Figure 9 shows the combustion characteristics of APC. Since the low-flow fuel injection maintains the minimum injection duration, the excess air coefficient of PC is closer to the premixed λ as the initial ambient pressure and λ increase. The peak heat release rate at the condition of λ=1.0&1.1 positively correlates with the increased ambient pressure. A turning point occurs when λ=1.2, and the peak heat release rate at 0.75 and 1.0MPa decreases rapidly as λ increases. When λ ≥ 1.3, the peak heat release rate is negatively correlated with changes in ambient pressure and a low ambient pressure of 0.5MPa shows higher peak heat release performance.

The difference in integral heat release in Figure 9(b) at different ambient pressure conditions gradually decreases as λ increases, indicating that the combustion heat release efficiency of high ambient pressure decreases faster than that of low ambient pressure. By converting the combustion efficiency with the stoichiometric ratio, the integral heat release percentage change value R_{HR} in Figure 9(b) can be the same as the PPC. The lean combustion efficiency of low ambient pressure jet ignition is improved at most conditions. The combustion efficiency improves the most when λ = 1.1, reaching 5.6%. When approaching the lean limit, the R_{HR} decreases. Relatively high ambient pressures of 0.75 and 1.0MPa will cause the lean combustion efficiency to continue to decrease. R_{HR} drops to the minimum value at various ambient pressure conditions when approaching the lean limit λ=1.5.

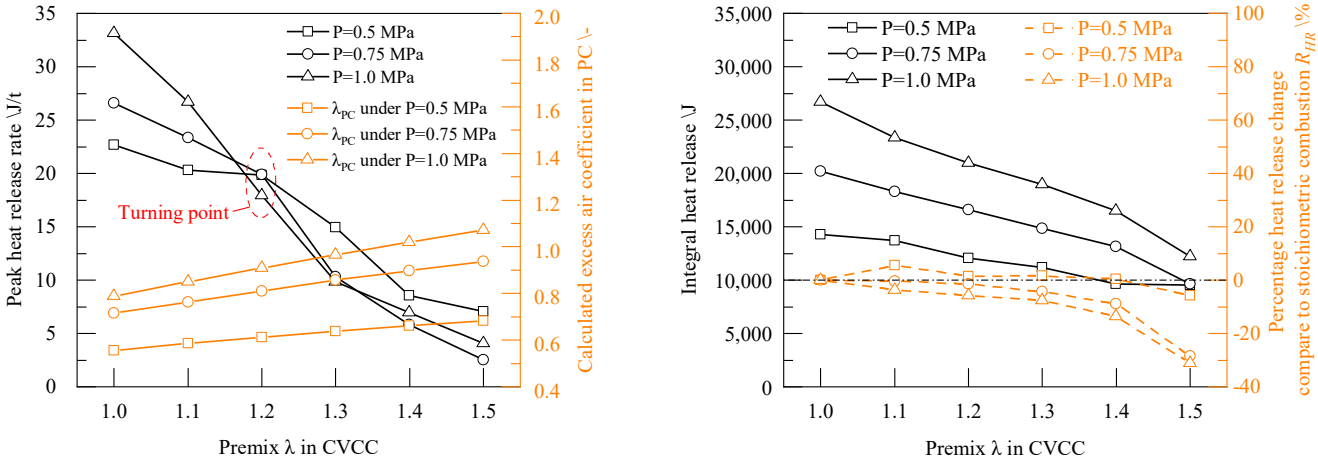

(a) Peak heat release (b) Integral heat release

Figure 9. Peak & integral heat release of APC.

Figure 10 shows the ignition delay period and main combustion period of APC. The ignition delay period increases as λ increases. Ignition delay at high ambient pressure of APC is mostly lower from stoichiometric to lean-combustion. This is due to the low energy of the premixed gas at low initial ambient pressure, and low-flow fuel injection enrichment in the PC leads to fuel enrichment, which reduces the flame propagation speed in the PC. At high ambient pressure conditions of 0.75 and 1.0 MPa, the fuel injection amount of 0.64 mg makes the excess air coefficient of PC closer to premixed λ. Hence, the ignition delay is lower than that of lower ambient pressure. Starting from λ = 1.4, lean combustion mainly affects ignition delay. Due to the significant reduction in heat release rate, the influence of ambient pressure on ignition delay no longer plays a dominant role. The ignition delay at lean conditions can be minimized by controlling the fuel concentration in the PC near the stoichiometric ratio when the combustion heat release is stable.

The main combustion period continues to increase as λ increases. At most operating conditions, the main combustion period of high ambient pressure at the same λ is higher than that at low ambient pressure, indicating that the main combustion period mainly depends on the premixed λ of the main chamber. Jet ignition only determines the flame propagation and combustion characteristics in the early stages of combustion.

 doi:10.20944/preprints202405.1648.v1

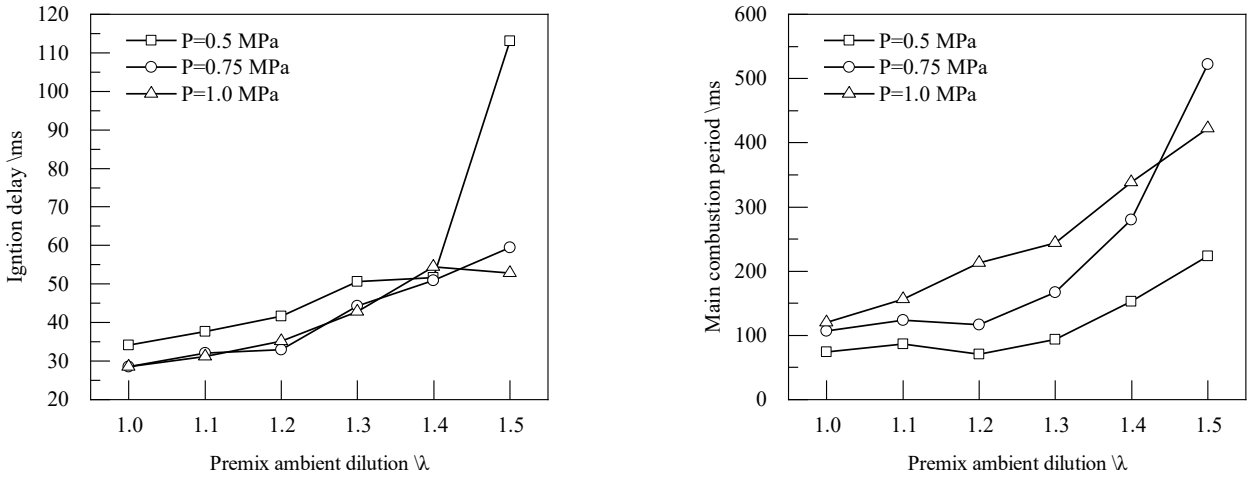

(a) Ignition delay (b) Combustion period

Figure 10. Combustion period of APC.

Figure 11 compares the combustion heat release performance of APC to PPC at different ambient pressure conditions. The APC has additional fuel consumption compared with the PPC. With the same low-flow fuel injection duration, the proportion of additional fuel consumption decreases as the ambient pressure increases, while it rises as λ increases. APC has achieved more significant performance gains than PPC in most combustion by adding a small proportion of 0.1% to 0.4% of additional fuel in the CVCC.

There are gains in peak heat release rate and integral heat release at various ambient pressure conditions. The peak heat release rate and integral heat release change simultaneously, and the heat release values of APC are higher than those of PPC. Combustion efficiency has the most significant improvement at low ambient pressure. When premixed λ is 1.1, the heat release performance of the PPC drops sharply due to the increase in ambient pressure. The APC has a more significant increase in heat release rate than the PPC.

Since the calculated theoretical λ_{PC} at the ignition time of APC belongs to the rich combustion range, the ignition delay period is generally longer than that of PPC. The ignition delay of the APC at low ambient pressure is higher than that of the PPC. Increasing the ambient pressure can shorten the ignition delay period. But compared with the PPC, APC significantly shortens the main combustion period at lean combustion.

At stoichiometric combustion conditions, the main combustion periods of the two jet ignition methods at various ambient pressures are not much different. As λ increases, the combustion performance of the APC begins to improve, and the main combustion period is significantly shortened. Compared with PPC, APC has a faster heat release rate and more stable combustion performance at the same premixed λ.

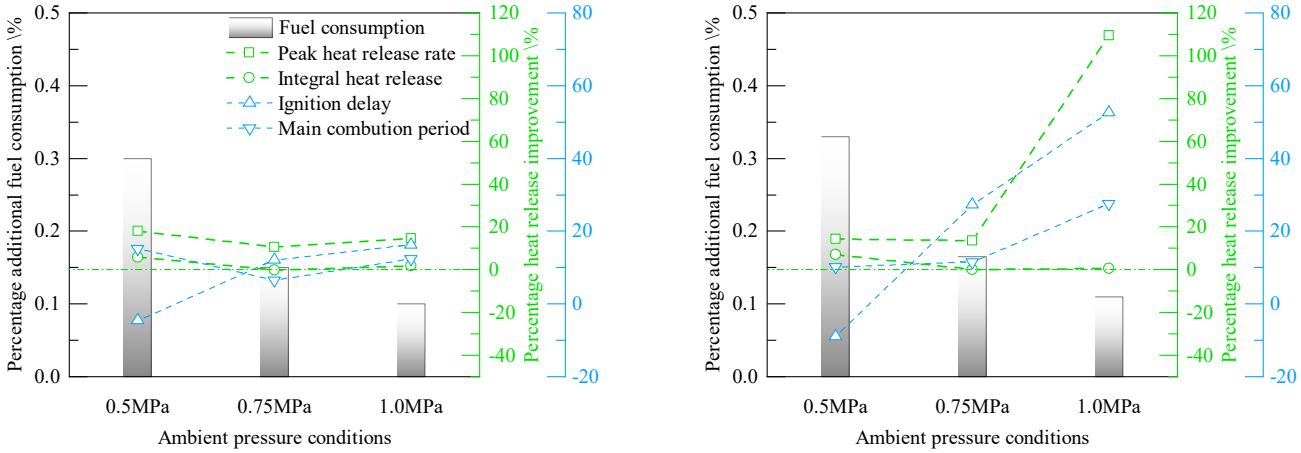

(a) λ=1.0 (b) λ=1.1

 doi:10.20944/preprints202405.1648.v1

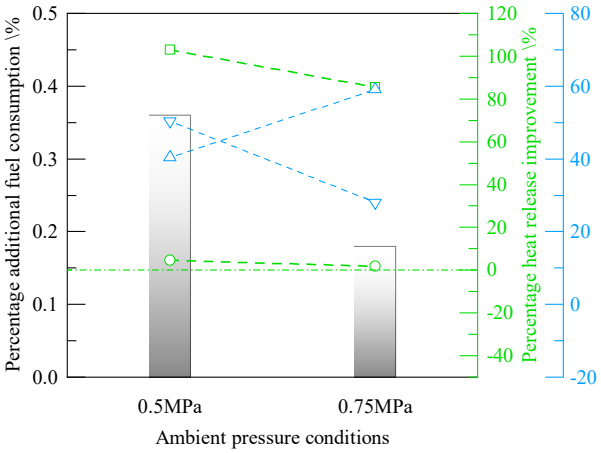

(c) λ=1.2

Figure 11. Improvement comparison to PPC.

3.2 Jet Flame Image Analysis

Figure 12 shows the flame images and flame analysis parameters of the PPC at stoichiometric combustion. The analysis starts with ignition timing. The jet flame area represents the flame propagation in the plane, while the jet length better represents the flame propagation in the jet direction.

The changes in flame propagation area at three different initial ambient pressure conditions are relatively close. At the condition of 1.0 MPa, the jet flame area increases rapidly in the initial stage, mainly related to the proper mixture state in the PC. The jet mixture concentration closer to the stoichiometric ratio brings a high-intensity jet flame, as shown in Figure 12 (c). The average penetration length of the jet is longer at the same time as the ambient pressure increases, indicating that the jet flame propagation velocity at high ambient pressure is faster in the initial stage of the jet ignition.

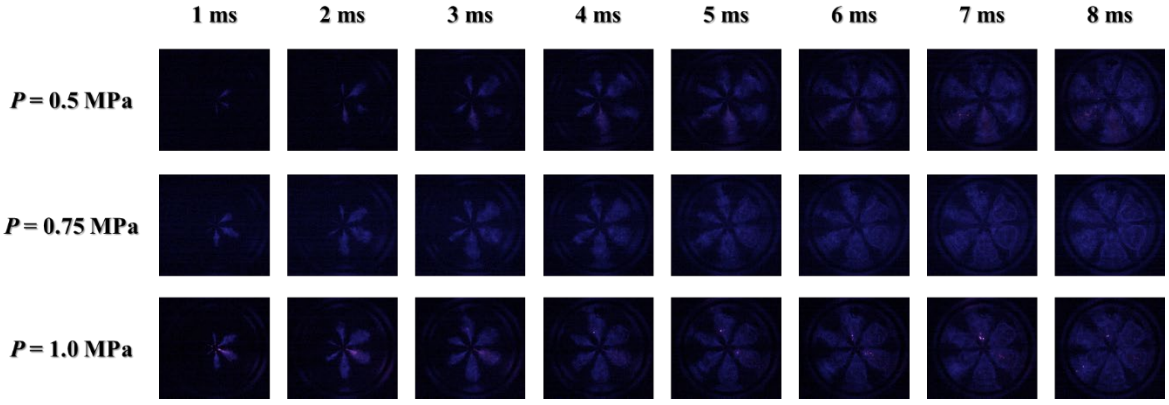

(a) Flame images

 doi:10.20944/preprints202405.1648.v1

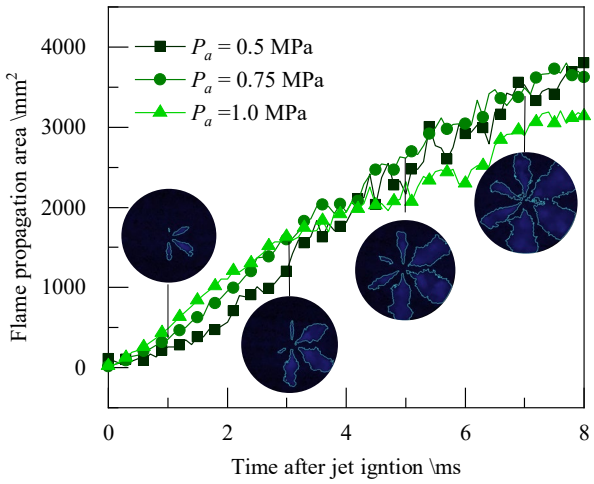

(b) Flame propagation area

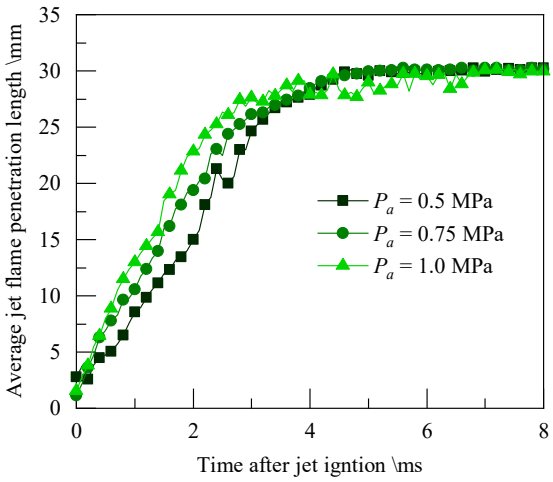

(c) Flame penetration length

Figure 12. Flame images & analysis at stoichiometric combustion of PPC.

At the condition of λ=1.1, the combustion intensity decreases, causing low-temperature combustion to dominate, and the brightness of the captured flame image is significantly weakened, as shown in Figure 13. The jet penetration length and flame area of 0.75 MPa ambient pressure is considerably higher than that of 0.5 MPa ambient pressure, which is consistent with the trend of heat release peak. The peak heat release rate at the maximum ambient pressure of 1.0 MPa is significantly lower than that during stoichiometric combustion, and the combustion state is already close to the lean limit at this ambient pressure condition. The λ significantly impacts the flame propagation intensity in the jet direction at high ambient pressure conditions and the turbulent diffusion entrainment propagation intensity of the in-plane jet flame. At the condition of λ=1.1, the PPC can no longer achieve good jet ignition and turbulent diffusion combustion performance at 1.0 MPa.

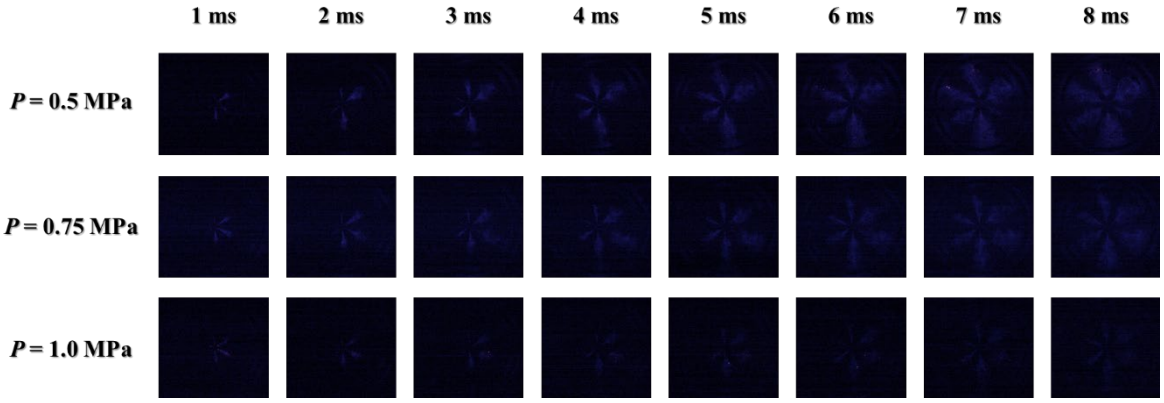

(a) Flame images

Preprints.org (www.preprints.org) | NOT PEER-REVIEWED | Posted: 24 May 2024 doi:10.20944/preprints202405.1648.v1

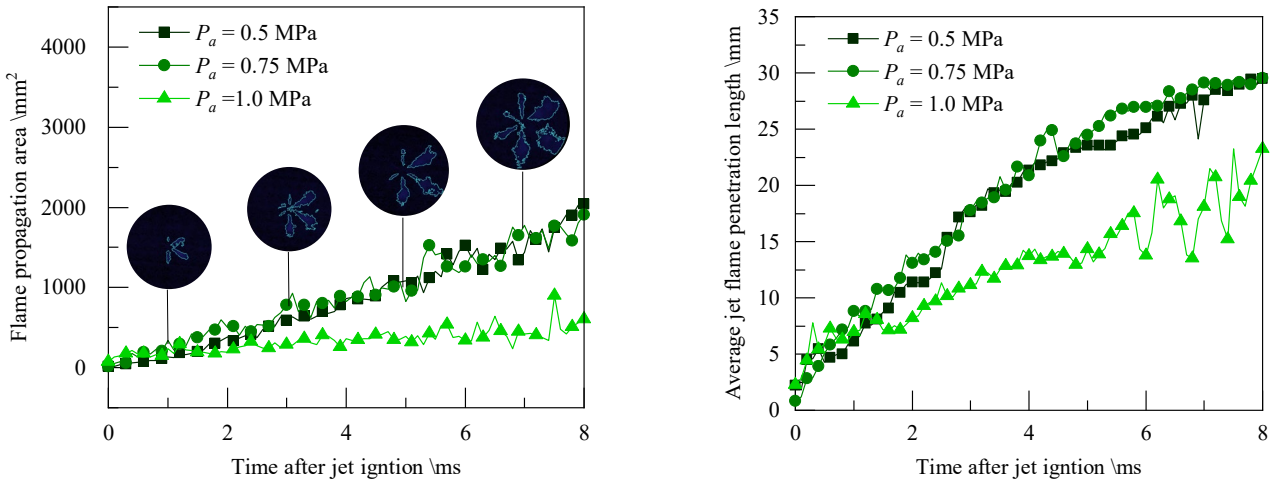

(b) Flame propagation area (c) Flame penetration length

Figure 13. Flame images & analysis at lean-combustion (λ=1.1) of PPC.

Figure 14 shows the calculated jet volume and jet flame entrainment change Φ of the PPC at different times. Stoichiometric combustion always maintains a larger jet flame volume than lean combustion, and the entrainment volume increases with the increase of the ambient pressure in the constant volume chamber. The higher the entrainment change Φ, the better the jet flame propagation and combustion heat release performance. When λ=1.1, due to the sharp decrease in the jet penetration length and flame propagation area at high ambient pressure conditions, the jet entrainment is also at the lowest level, resulting in the jet ignition at 1.0 MPa condition being in close to the lean combustion limit.

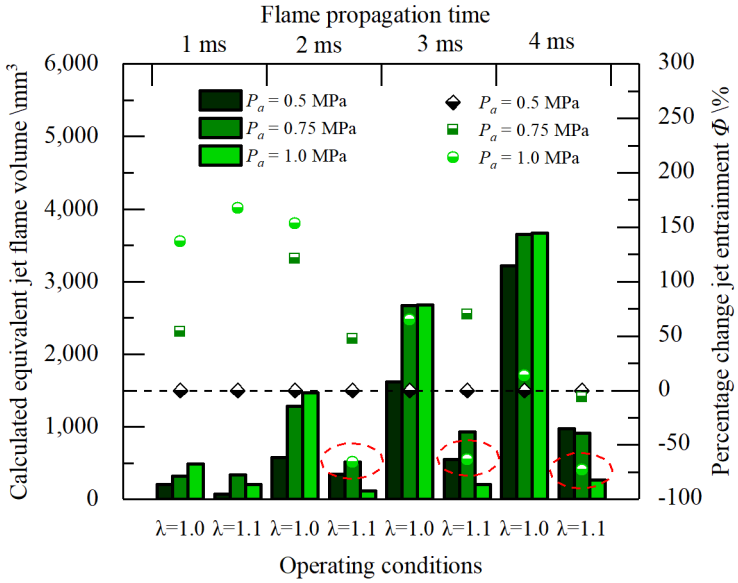

Figure 14. Calculated jet volume and jet flame entrainment change.

Figure 15 shows the flame propagation images, flame area, and jet penetration of APC stoichiometric combustion. Through the additional low-flow fuel injection in the pre-chamber, the image's overall brightness in the jet phase is significantly increased compared to that of PPC. Although the pre-chamber is in a fuel-enriched state, the energy intensity of the jet still increases significantly.

Similar to the changes in the PPC, at stoichiometric combustion conditions, the jet area with a high ambient pressure of 1.0MPa has the highest growth rate in the early stage, and the difference in area change is mainly concentrated in the jet propagation stage. After the jet flame front reaches the

 doi:10.20944/preprints202405.1648.v1

optical limit of the window, the difference in area change gradually decreases, especially because the jet flame of high ambient pressure condition has the highest velocity, and the flame propagates quickly in the direction of the jet.

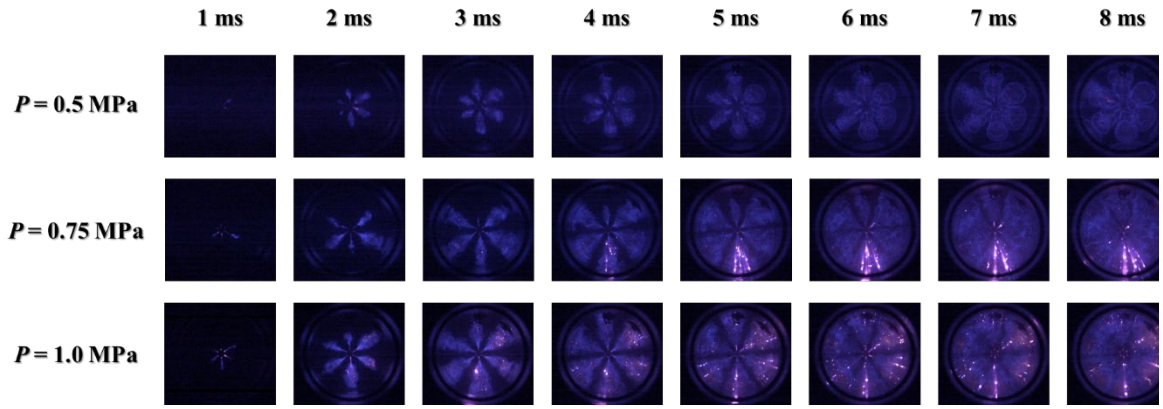

(a) Flame images

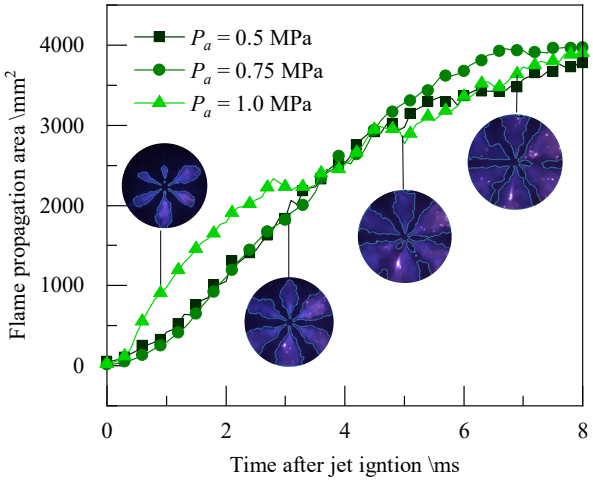

(b) Flame propagation area

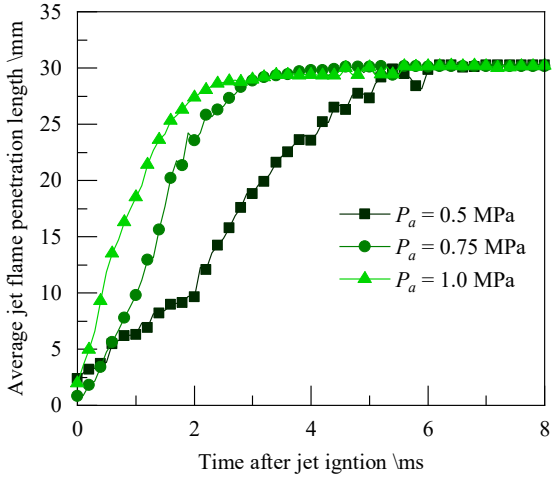

(c) Flame penetration length

Figure 15. Flame images & analysis at stoichiometric combustion of APC.

Figure 16 below shows the flame images area, and jet penetration of the APC at λ=1.2. The peak heat release rate trend is consistent with the jet penetration velocity trend at different ambient pressures. The main reason for the heat release is the flame jet intensity, and the jet penetration is a direct reflection of the jet flame intensity.

Compared with stoichiometric combustion in APC, the difference in jet penetration between different ambient pressure conditions decreases, and the difference in area change increases. It shows that the difference in flame propagation area is mainly in the circumferential direction and is closely related to the jet flame shape during the jet development process. At the condition of λ=1.2, the peak heat release is the lowest at 1.0 MPa. However, it still maintains a jet penetration length and speed higher than 0.5MPa, which means that additional fuel injection in the active pre-chamber can improve the flame propagation in the jet direction even at high ambient pressure.

 doi:10.20944/preprints202405.1648.v1

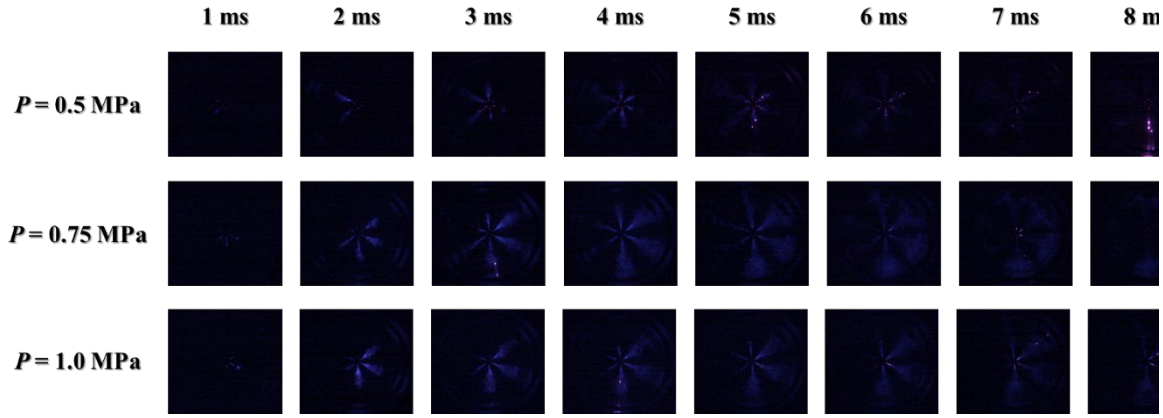

(a) Flame images

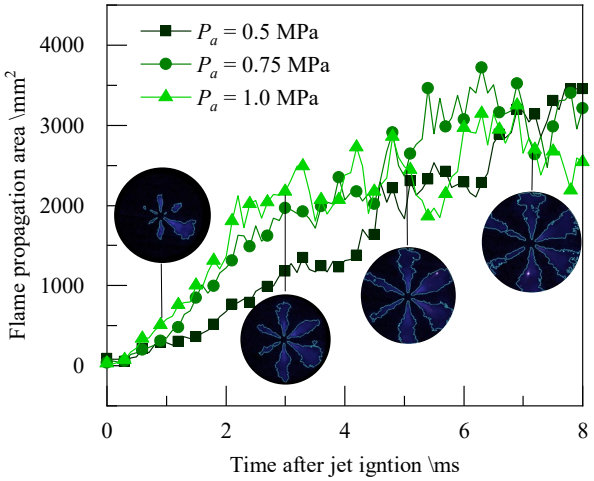

(b) Flame propagation area

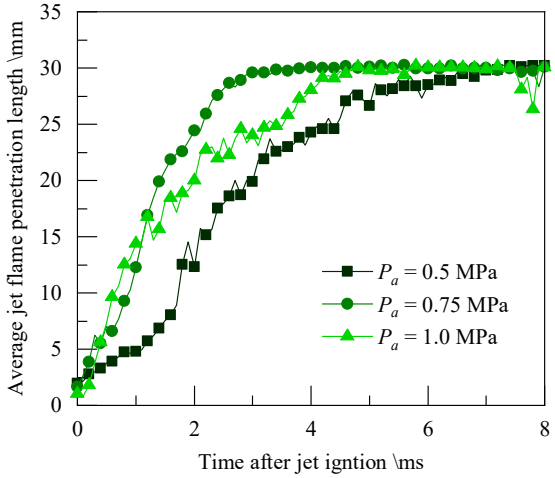

(c) Flame penetration length

Figure 16. Flame images & analysis at lean-combustion (λ=1.2) of APC.

Figure 17 shows the evolution of the flame profile at different ambient pressures at λ=1.2. At high ambient pressure of 1.0MPa, combustion heat release performance decreases, jet velocity decreases, and uniformity worsens. Due to the weak entrainment ability of the flame area, the circumferential propagation speed slows down. Although the jet entrainment volume is directly related to the jet velocity, the effect of high ambient pressure dominates. The result of ambient pressure on jet flame propagation is mainly reflected in transforming a wide jet flame into a narrow jet flame, thereby prolonging the in-plane flame propagation time.

 doi:10.20944/preprints202405.1648.v1

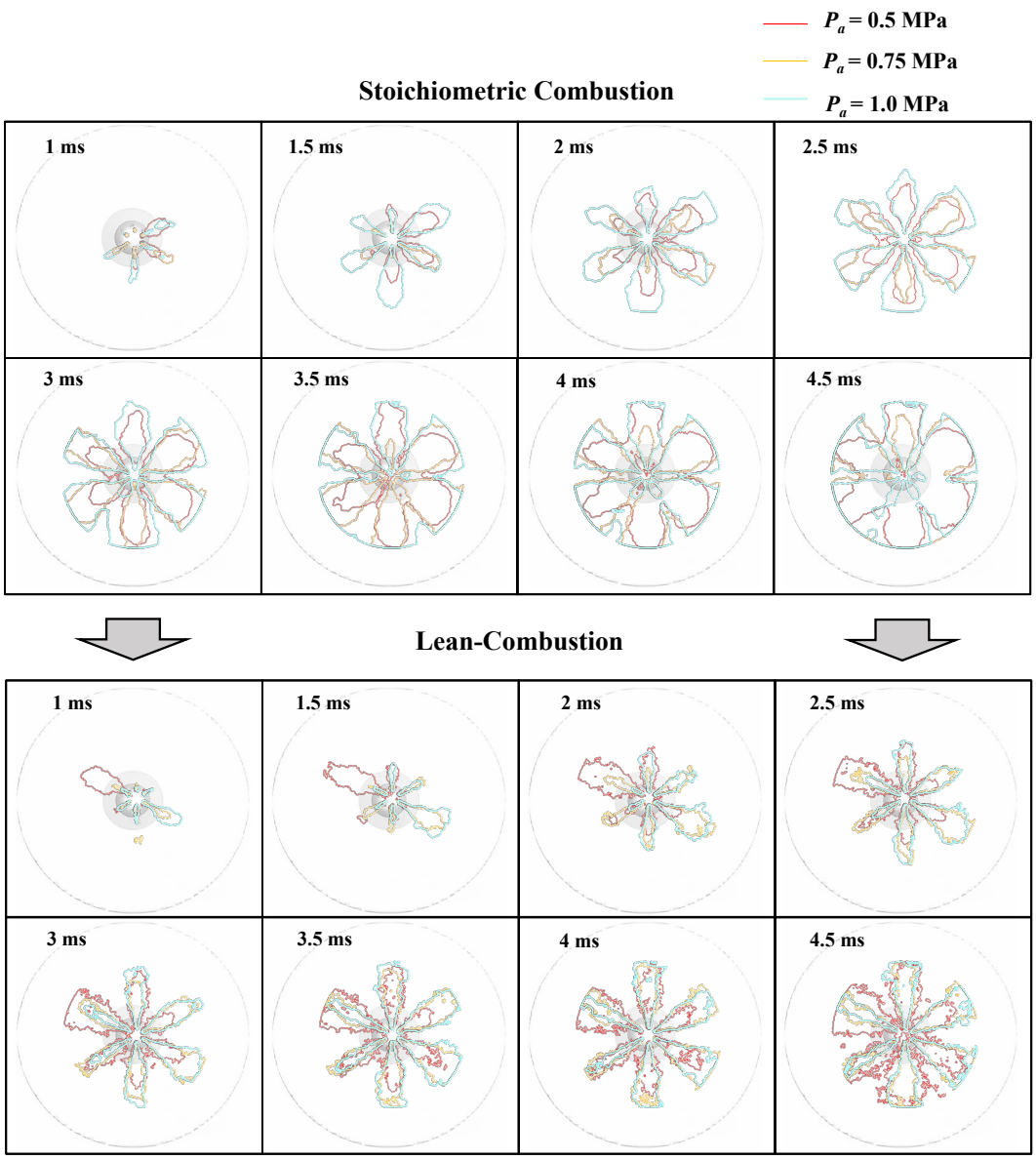

Figure 17. Jet flame contour of different ambient pressure.

Figure 18 shows the jet volume and entrainment change Φ calculated at different times. At the combustion condition of stoichiometric ratio λ = 1.0, the jet flame volume increases significantly as the ambient pressure increases, and the change rate of entrainment volume at high ambient pressure relative to the low ambient pressure of 0.5MPa is positive. At lean combustion conditions, the initial jet flame entrainment volume at high ambient pressure increases the jet intensity due to the additional low-flow fuel injection, and the entrainment volume change rate is higher than that at 0.5MPa low ambient pressure. With the jet flame's development, the jet flame's volume at the condition of 1.0MPa at 3ms and 4ms after jet flame ignition in CVCC has been less than that of 0.5 MPa. The change rate of the entrainment amount has become negative simultaneously.

Preprints.org (www.preprints.org) | NOT PEER-REVIEWED | Posted: 24 May 2024 doi:10.20944/preprints202405.1648.v1

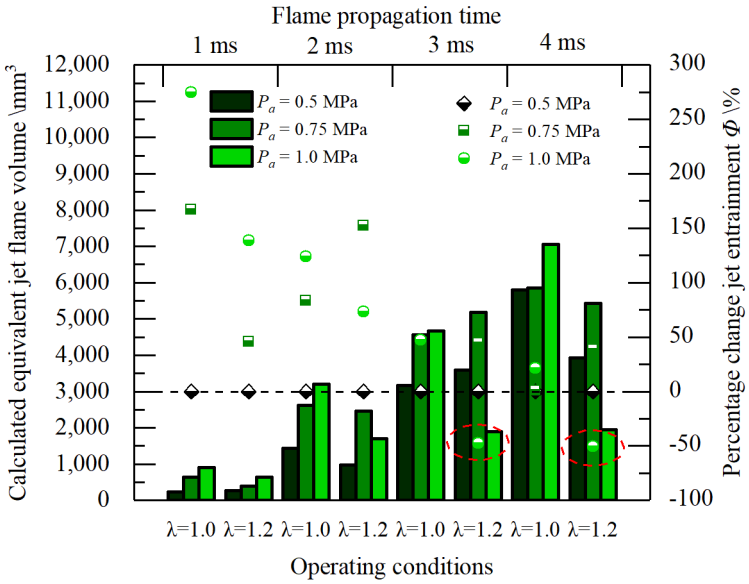

Figure 18. Equivalent jet volume and percentage entrainment change of different ambient pressures.

4. Conclusions

This paper studied the effect of initial ambient pressure on APC and PPC with a constant volume combustion chamber. The heat release rate, IHR, heat release change ratio, flame area, jet flame propagation length, and percentage change jet entrainment were used to investigate the combustion and flame propagation characteristics. The main conclusions are as follows:

1. The APC could expand the lean limit to premixed λ=1.5 compared with premixed λ=1.2 of PPC at different ambient pressures.
2. At stoichiometric and slightly lean combustion conditions, appropriately increasing the ambient pressure can promote ignition and combustion performance of APC and PPC with the heat release peak increased and the combustion period shortened. At lean combustion conditions, the ignition and combustion performance decrease rapidly after the premixed λ exceeds a certain value at high ambient pressure, while APC could increase the premixed λ corresponding to this turning point.
3. At the stoichiometric combustion and slightly lean combustion (λ=1.0 and λ=1.1) conditions with APC, the peak heat release rate positively correlates with the initial ambient pressure increase. As the premixed λ increases, the peak heat release rate and ambient pressure negatively correlate.
4. The ignition delay increases with the increase of premixed λ. At the same time, the ignition delay period of APC is directly related to the fuel concentration in the PC. The ignition delay can be minimized by controlling the excess air coefficient in the pre-chamber near the stoichiometric ratio.
5. The high initial ambient pressure in the constant-volume chamber dramatically reduces the volume of the jet flame and the mixture entrainment capacity at lean-combustion conditions, thereby reducing the combustion speed and peak heat release. At the same time, the APC can significantly increase the jet intensity, which could weaken the ambient pressure effect on the jet penetration at lean combustion conditions.

 doi:10.20944/preprints202405.1648.v1

Abbreviations

	R_{HR}	Combustion heat release change ratio
	Q	Integral heat release rate
	Q_{sto}	Integral heat release rate at stoichiometric combustion condition
	m	Fuel injection mass
	m_{sto}	Fuel injection mass at stoichiometric combustion condition
	$\overline{X}$	The average jet flame penetration length
X’		The jet length in the axis direction
S		The cumulative flame area
R		The approximate spherical radius
	V_{Jet}	The equivalent jet flame volume
	V_{Jet0}	The jet flame volume of stoichiometric combustion at 0.5 MPa initial ambient pressure
	Φ	Percentage change rate of the jet flame volume
APC		Active pre-chamber
CVCC		Constant-volume combustion chamber
HEI		High-energy spark ignition
MCP		Main chamber combustion period
PC		Pre-chamber
PPC		Passive pre-chamber

Author Contributions: Minglong LI: Software, Methodology, Validation, Investigation, Formal analysis, Visualization, Writing - Original Draft, Writing - Review & Editing Zongjie HU: Conceptualization, Supervision, Funding acquisition, Writing - Review & Editing Xinke MIAO: Investigation, Funding acquisition, Writing - Review & Editing Yuanzhi WANG: Investigation, Funding acquisition, Writing - Review & Editing Xijiang WU: Investigation, Funding acquisition, Writing - Review & Editing Wangchao YU: Investigation, Writing - Review & Editing Yuanzhi TANG: Investigation, Formal analysis, Writing - Original Draft, Writing - Review & EditingZhe KANG: Writing - Review & Editing Jun DENG: Conceptualization, Supervision, Funding acquisition, Writing - Review & Editing

Acknowledgment: This research was funded by the National Natural Science Foundation of China (No. 52076153), the Shanghai Science and Technology Program (No. 22ZR1463000), the projects in Science and Technique Plans of Ningbo City (No.2022Z023) and the National Key R&D Program of China (2021YFB2500800).

Conflict of Interest: The authors declare that they have no known competing financial interests or personal relationships that could have appeared to influence the work reported in this paper.

 doi:10.20944/preprints202405.1648.v1

References

1. Toulson, E., Schock, H., and Attard, W., "A Review of Pre-Chamber Initiated Jet Ignition Combustion Systems," SAE Technical Paper 2010-01-2263, 2010. Doi:10.4271/2010-01-2263.
2. Joshi, A., "Review of Vehicle Engine Efficiency and Emissions," SAE Int. J. Adv. & Curr. Prac. in Mobility 2(5):2479-2507, 2020, Doi:10.4271/2020-01-0352.
3. Atis, C., Chowdhury, S., Ayele, Y., Stuecken, T. et al., "Ultra-Lean and High EGR Operation of Dual Mode, Turbulent Jet Ignition (DM-TJI) Engine with Active Pre-chamber Scavenging," SAE Technical Paper 2020-01-1117, 2020, Doi:10.4271/2020-01-1117.
4. Ayala, F., Gerty, M., and Heywood, J., "Effects of Combustion Phasing, Relative Air-fuel Ratio, Compression Ratio, and Load on SI Engine Efficiency," SAE Technical Paper 2006-01-0229, 2006, Doi:10.4271/2006-01-0229.
5. Li, F., Wang, Z., Wang, Y. et al. High-Efficiency and Clean Combustion Natural Gas Engines for Vehicles. Automot. Innov. 2, 284–304 (2019). Doi:10.1007/s42154-019-00075-z.
6. Jamrozik, Arkadiusz and Wojciech Tutak. “A study of performance and emissions of SI engine with a two-stage combustion system.” Chemical and Process Engineering 32 (2011): 453-471. Doi: 10.2478/v10176-011-0036-0.
7. Jiaye Shi,Jinqiu Wang,Jun Deng,Xinke Miao,Yihui Liu,Liguang Li. Study on Combustion and Emission Characteristics of High Compression Ratio Gasoline Engine Based on Two‐stage High Energy Ignition and Passive Pre‐chamber[J]. Automotive Engineering, 2021, 43(9): 1300-1307. Doi: 10.1016/j.energy.2023.127398.
8. Wimmer, D. and Lee, R., "An Evaluation of the Performance and Emissions of a CFR Engine Equipped with a Prechamber," SAE Technical Paper 730474, 1973, Doi:10.4271/730474.
9. WU Jian, CHEN Jiawen, DU Jiakun, CHEN Hong, LI Yuhuai, ZHAN Wenfeng. Combustion and Emission Characteristics of a Lean Burn Gasoline Direct Injection Engine with Active Pre-chamber. Chinese Internal Combustion Engine Engineering, 2021, 42(3): 55-60.
10. Attard, William P., Neil Fraser, Patrick Parsons and Elisa Toulson. “A Turbulent Jet Ignition Pre-Chamber Combustion System for Large Fuel Economy Improvements in a Modern Vehicle Powertrain.” SAE International journal of engines 3 (2010): 20-37. DOI: 10.4271/2010-01-1457
11. Zheng, Zeyuan, Lei Wang, Jiaying Pan, Mingzhang Pan, and Haiqiao Wei. “Numerical Investigations on Turbulent Jet Ignition with Gasoline as an Auxiliary Fuel in Rapid Compression Machines.” Combustion Science and Technology 195, no. 4 (2023): 672–91. Doi:10.1080/00102202.2021.1969375.
12. Yang X, Cheng Y, Zhao Q, Wang P, Chen J. Effect of spark ignition location on the turbulent jet ignition characteristics in a lean burning natural gas engine. International Journal of Engine Research. 2023;24(2):702-719. Doi:10.1177/14680874211064677.
13. Qiang Wang, Longhua Hu, Suk Ho Chung. Blow-out of nonpremixed turbulent jet flames at sub-atmospheric pressures. Combustion and Flame, 2017(176):358-360. Doi:10.1016/j.combustflame.2016.11.016..
14. Hee J. Kim, Kyuho Van, Dae K. Lee, Chun S. Yoo, Jeong Park, Suk H. Chung. Laminar flame speed, Markstein length, and cellular instability for spherically propagating methane/ethylene–air premixed flames. Combustion and Flame, 2020(214):464-474, Doi:10.1016/j.combustflame.2020.01.011.
15. Shah, a., p. Tunestal, and b. Johansson. Effect of relative mixture strength on performance of divided chamber ‘avalanche activated combustion’ ignition technique in a heavy duty natural gas engine. SAE Technical Paper, 2014-01-1327, 2014 Doi:10.4271/2014-01-1327.
16. Busch, S., Bohac, S. V., and Assanis, D. N. (June 6, 2008). "A Study of the Transition Between Lean Conventional Diesel Combustion and Lean, Premixed, Low-Temperature Diesel Combustion." ASME. J. Eng. Gas Turbines Power. September 2008; 130(5): 052804. Doi.org/10.1115/1.2906177.
17. Deng Jun, Zhong Huiping, Gong Yinchun, Gong Xuehai, Li Liguang. Studies on injection and mixing characteristics of high pressure hydrogen and oxygen jet in argon atmosphere. Fuel. 2018(226). 454-461. Doi:10.1016/j.fuel.2018.04.038.